Characterization of Semi-insulator Devices in Electrophotography with Corona Charging Current Measurements

Inan Chen and Ming-Kai Tse
Quality Engineering Associates (QEA), Inc., Burlington, Massachusetts, USA

Abstract

The "Electrostatic Charge Decay" (ECD) technique, previously introduced for electrical characterization of semi-insulating devices in electrophotography, involves open-circuit <u>voltage</u> measurements of corona charged layer as a function of time and/or position. The interpretation of data is based on first-principle charge transport theory. This provides information more relevant to the performance of the devices in electrophotographic applications. In the present work, the technique is extended by including the measurements of corona charging <u>currents</u>. The steady state values of charging current allow a more precise determination of charge injection properties. In addition, the key parameters can be consolidated into an effective resistance that can be used as a figure of merit for routine quality control purposes. Representative examples of characterization are presented for demonstration.

Introduction

In electrophotography, the performance of charging and development rolls, transfer media, and charge transport layer of photoreceptors depends critically on the nature of dielectric relaxation in the polymeric semi-insulating composite materials constituting the devices.[1-4] The inhomogeneity and low purity of the composite material often introduce features such as non-Ohmic charge injection and field dependent mobility. Consequently, electrical characterization of such materials requires more than the traditional concept of conductivity.[5] The large area of these devices requires spatial uniformity of the charge transport properties to be monitored efficiently. To closely simulate the actual electrophotographic applications of the devices and to yield more relevant information on the device performance, characterization has to be performed under the non-constant voltage, open-circuit condition.

The "Electrostatic Charge Decay" (ECD) technique, which we introduced previously,[1-4,6,7] has almost fulfilled these objectives. The technique involves open-circuit <u>voltage</u> measurements of corona charged layer as a function of time and/or position, combined with data interpretation based on first-principle charge transport theory. It has been demonstrated experimentally and theoretically that the ECD technique can provide information more relevant to device performance in electrophotographic applications than the traditional closed circuit resistance measurements combined with interpretations based on equivalent RC circuit equations. However, because of the large number of transport parameters involved, additional measurements are needed for a complete characterization. It is also desirable to consolidate the key parameters into a simple figure of merit for routine applications. For this purpose, we extend the measurements to include the corona charging <u>currents</u>. (US patent pending, QEA, Inc.)

The experimental setup for the extended ECD technique for voltage and current measurements is shown schematically in Fig. 1.
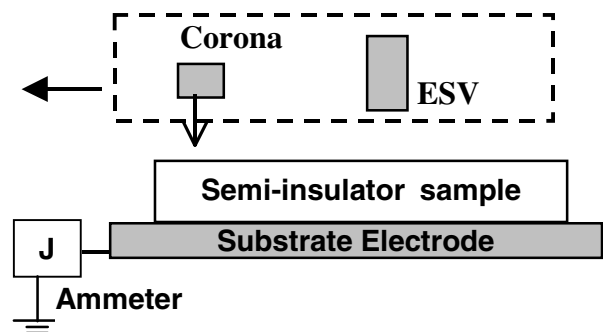

Figure 1. Schematic of experimental setup for voltage and current measurements in extended Electrostatic Charge Decay (ECD) technique

An important merit of current measurements is the fact that the currents can be measured simultaneously with corona charging. In contrast, the voltages can only be measured at a period of time after the termination of charging, because the corona source and the voltage probe (ESV) have to be spatially separated. For samples with higher conductivity (e.g. transfer media), the voltage decay during charging is significant, and provides important information.

Theoretical Background

The mathematical model for the voltage and current based on first principle charge transport theory has been described previously.[3,5] It is assumed that the sample thickness L and permittivity ε are known or can be estimated to within a sufficient accuracy. The variation of corona current J_C with the surface voltage V_s can usually follows the empirical linear relation:

$$J_C = J_{mx}(1 - V_s/V_{mx}) \qquad (1)$$

where J_{mx} is the initial (maximum) current at $V_s = 0$, and V_{mx} is the cut-off voltage at $J_C = 0$.

The sample is electrically characterized by the intrinsic charge density q_i and the positive and negative charge mobilities, μ_p and μ_n. These quantities are related to the conductivity by $\sigma = q_i(\mu_p + \mu_n)$. The mobilities are, in general, field dependent, and for simplicity, represented by the power law, $\mu(E) = \mu_m(E/E_m)^\omega$, where μ_m is the mobility at a field E_m (e.g. chosen as V_{mx}/L), and ω is the power. μ_m and ω may have different values for positive and negative charges.

The injection currents from the corona ions at the surface ($x = 0$) and that from the substrate electrode ($x = L$) are assumed to be proportional to the local field $E(0)$ and $E(L)$, respectively,

$$J_{inj}(0) = s_0 E(0) \text{ and } J_{inj}(L) = s_1 E(L) \qquad (2)$$

where s_0 and s_1 are two parameters (with the dimension of conductivity) that specify the charge injection properties of the interfaces.

Examples of charging currents vs. time curves calculated from the above charge transport model are shown in Fig. 2. All variables are expressed in normalized units defined below, with the typical values of these units given in parenthesis:

Current density: $J_o = J_{mx}$ ($\approx 10^{-5}$ A/cm^2)

Voltage: $V_o = V_{mx}$ ($\approx 10^3$ V)

Resistance: $R_o = V_o/J_o$ ($\approx 10^8$ Ωcm^2)

Capacitance: $C = \varepsilon/L$ ($\approx 3 \times 10^{-11}$ F/cm^2)

Time: $t_o = R_o C = C V_o/J_o$ ($\approx 3 \times 10^{-3}$ sec)

Conductivity: $\sigma_o = L/R_o = J_o L/V_o$ ($\approx 10^{-10}$ S/cm)

Charge density: $q_o = C V_o/L$ ($\approx 3 \times 10^{-6}$ C/cm^3)

Mobility: $\mu_o = \sigma_o/q_o$ ($\approx 3 \times 10^{-5}$ cm^2/Vsec) $\qquad (3)$

In the examples of Fig. 2, μ_p and μ_n are assumed to be equal and field-independent ($\omega = 0$). Three values of intrinsic charge density $q_i = 0$, 1 and 10 in units of q_o, and two values of injection parameters, with $s_0 = s_1 = 0.1$ and 1, in units of σ_o are considered.
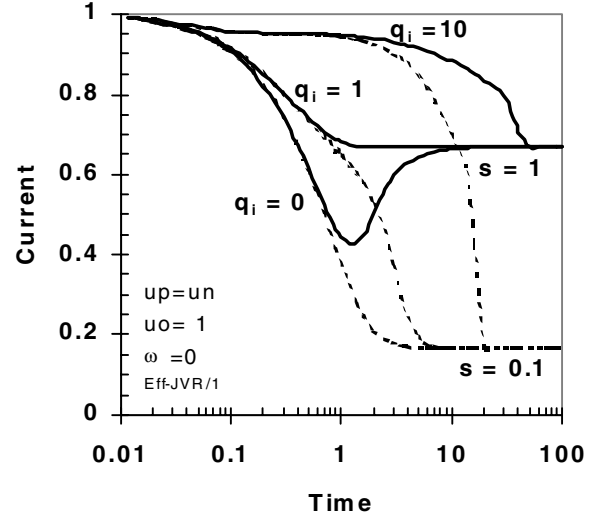

Figure 2. Calculated time evolution of charging currents.

It can be seen from Fig. 2 that although it takes longer to reach the steady state for samples with larger intrinsic charge densities q_i, the steady state currents J_{ss} are independent of q_i, and are determined by the injection parameters (s_0, s_1) only. Similar calculations with asymmetric injection ($s_0 \neq s_1$), unequal and/or field dependent mobilities ($\mu_p \neq \mu_n$, $\omega \neq 0$) yield the same conclusion. Thus, the steady state current is a good measure of the injection property of the interface.
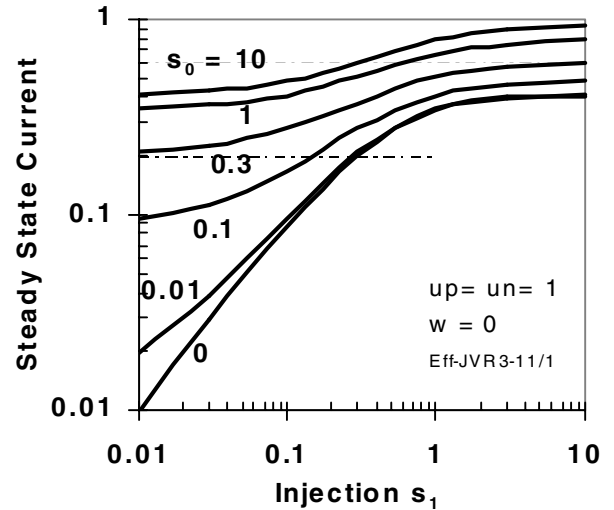

Figure 3. Steady state values of charging currents calculated for various values of injection parameters s_0 and s_1, defined in Eq.(2).

The steady state currents J_{ss} calculated from the mathematical model for various combinations of the injection parameters (s_0, s_1) are summarized in Fig. 3. In this figure, J_{ss} is plotted as a function of the injection parameter s_1, for a given value of s_0. As in Fig. 2, the mobilities are

assumed $\mu_p = \mu_n$ and field independent. Qualitatively similar curves are obtained with field dependent and unequal mobilities.

Using the measured values of J_{SS} and the knowledge on the relative size of injection from both interfaces, one can determine the injection parameters from the curves in Fig. 3 (or similar ones for different mobilities). For example, suppose the measured steady state current is $J_{SS} = 0.2J_{mx}$ (as shown by one of the dashed lines in Fig. 3). Then, from the curves in Fig. 3, one can deduce that either (a) one of the interface injection is very small $s_0 \approx< 0.01$ and the other is $s_1 \approx 0.3$, or (b) both $s_0 \approx s_1 \approx 0.1$, in units of σ_o defined in Eq.(3). Alternatively, suppose the measured value is $J_{SS} = 0.6$, then, both of the injection parameters are $s > 0.3\sigma_o$.

Concurrent with the charging current reaching the steady state, the surface voltage also reaches a steady state value, V_{SS}. As mentioned before, this voltage cannot be measured with conventional electrostatic voltage probes (as shown in Fig.1) because of mutual spatial exclusion with the charging corona device. However, the voltage and current during corona charging are related by the empirical corona characteristics, Eq.(1). Thus, V_{SS} can be calculated from the measured J_{SS}. Then, an effective resistance can be defined by,

$$R_{eff} = V_{SS}/J_{SS} \qquad (4)$$

and the steady state can be described by an equivalent circuit with the sample represented by the effective resistance R_{eff} and the capacitance C in parallel as shown by the inset in Fig. 4. Solving the equivalent circuit equation,

$$C(dV/dt) + V/R_{eff} = J_C = J_{mx}(1 - V/V_{mx}) \qquad (5)$$

one obtains,

$$V(t) = J_{mx}R_X[1 - exp(-t/CR_X)] \qquad (6)$$

$$J(t) = J_{mx}(R_X/R_{eff})[1 + (R_{eff}/R_o)exp(-t/CR_X)] \qquad (7)$$

where $R_X = R_{eff}R_o/(R_{eff} + R_o)$ and $R_o = V_{mx}/J_{mx}$ is the unit defined in Eq.(3). It can be seen that in the steady state ($t \to \infty$), the ratio $V_{SS}/J_{SS} = V(\infty)/J(\infty)$ is equal to R_{eff}. Furthermore, from Eq.(7) one has,

$$J_{SS} = J(\infty) = J_{mx}/(1 + R_{eff}/R_o),$$

or, $$R_{eff}/R_o = J_{mx}/J_{SS} - 1 \qquad (8)$$

This relation is shown in Fig. 4, and provides a way to determine R_{eff} from the measured J_{SS} value. It should be reminded that the R_{eff} value determined by this technique is a measure of the injection properties and is independent of the conductivity or intrinsic charge density. Therefore, the value can be significantly different from that expected from the nominal conductivity or resistivity of the sample, but is more relevant to applications of the present interest.

Experimental Results and Discussion

The application of this technique is demonstrated below by the examination of charge injection into typical plain paper samples. In order to examine the sensitivity of R_{eff} values to different injection conditions, the same plain paper sample is tested with and without an injection-blocking thin insulator interposed between the sample and the sources of injecting charges.
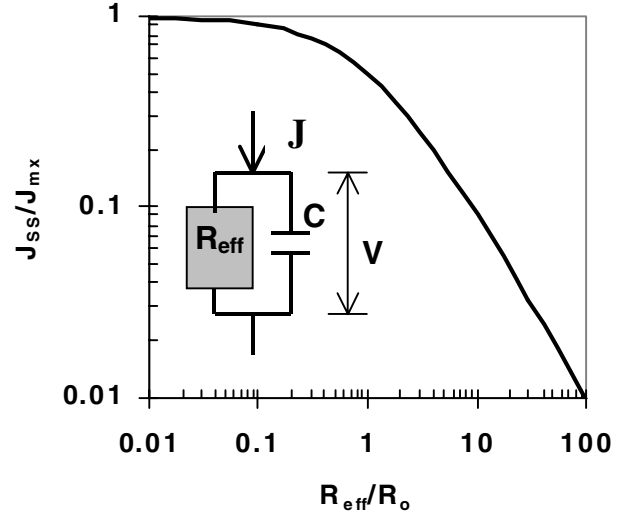

Figure 4. Variation of steady state currents J_{SS} with the effective resistance R_{eff}, Eq. (8). J_{SS} and R_{eff} are normalized to the units J_{mx} and R_o, respectively, defined in Eq.(3). The inset shows the equivalent circuit for the steady state under corona charging.
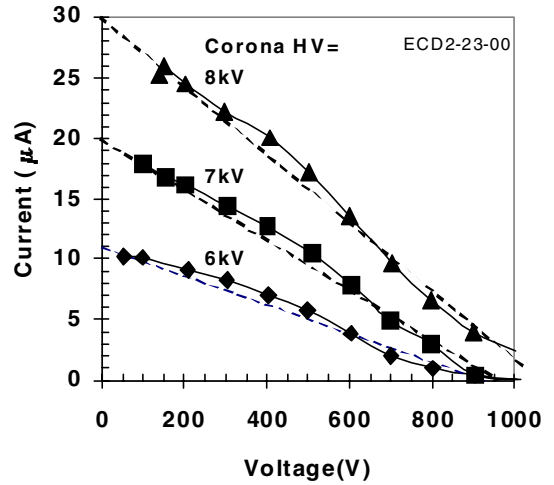

Figure 5. Corona charging characteristics measured at three values of wire voltage 6, 7, and 8kV.

The current-voltage characteristics of corona charger used in this experiment are shown in Fig. 5, for three settings of corona wire voltage (6, 7 and 8 kV). These curves are used to obtain the empirical relation Eq.(1) and then, V_{SS} from measured J_{SS} values.

The measured J_{ss} values are shown in Fig. 6 for the three injection conditions: (a) without any blocking layer, (b) with a blocking layer at the (bottom) interface with the substrate electrode, and (c) with blocking layers on both interfaces. The R_{eff} values that are calculated from these J_{ss} and the corresponding V_{ss} (from Fig. 5) are shown in Fig. 7 for the three cases.
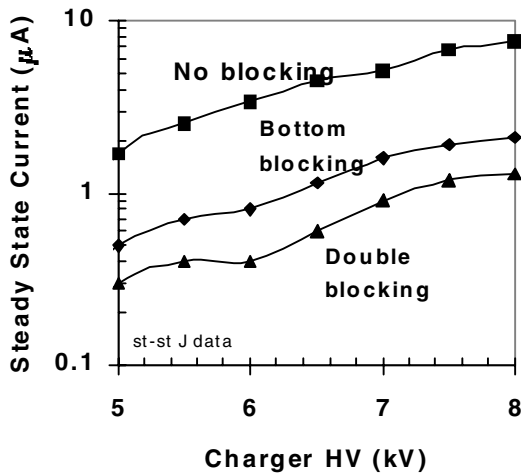

Figure 6. Steady state currents measured at varying charger wire voltages, under three different injection conditions.
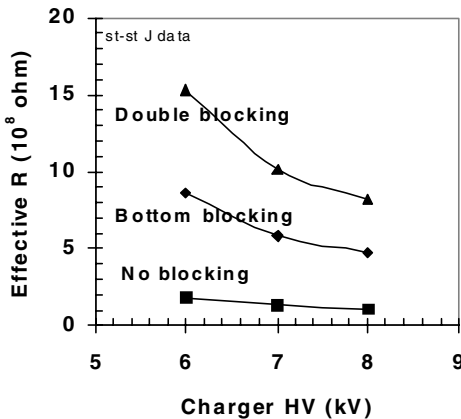

Figure 7. Effective resistance determined for the three injection conditions from measured steady state currents of Fig. 6.

It can be seen that for each corona setting, the deduced R_{eff} values increase as additional blocking layers are introduced, in spite of the fact that the same paper samples are used in the tests. This indicates that, the R_{eff} values deduced from the measurements of steady state currents as described above do reflect the charge injection properties at the interface. It also demonstrates the important role played by charge injection in dielectric relaxation of semi-insulator samples.

Summary and Conclusions

The traditional ECD technique with voltage measurements has been extended to include charging current measurements. This enables the determination of charge injection properties at the interfaces, which is an important characteristic for device performance. From the measured steady state currents, the injection properties are characterized in terms of two parameters s_0 and s_1 that have the dimension of conductivity, or more conveniently by an effective resistance R_{eff} that is solely determined by injection and not related to bulk resistivity.

References

1. M.-K. Tse, D. J. Forest, and F. Y. Wong, Predicting charge roller performance in electrophotography using electrostatic charge decay measurements, *Proc. IS&T's NIP-11*, pg.383 (1995)
2. M.-K. Tse and I. Chen, The role of dielectric relaxation in charge roller performance, *Proc. IS&T's NIP-14*, pg.481 (1998)
3. I. Chen and M.-K. Tse, The role of dielectric relaxation in media for electrophotography (I) Modeling of electrostatic transfer, *Proc. of IS&T's NIP-15*, pg. 155 (1999)
4. I. Chen and M.-K. Tse, Electrical characterization of transfer media for electrophotography, *Proc. of IS&T's NIP-16*, pg. 208 (2000)
5. I. Chen and M.-K. Tse, Electrical characterization of semi-insulating devices for electrophotography, *Proc. IS&T's NIP-15*, pg. 486, (1999); also in *J. Imag. Sci. & Tech.,* 44, 462 (2000)
6. M.-K. Tse et al. Automated Stationary/Portable Test System for Photoconductive Drums, US Patent, 5,929,640 (1999); N.P.Suh and M.-K.Tse, A new NDE technique for composites. US Patents, 4,443,764 (1984)
7. M.-K. Tse, Quality control test equipment for photoreceptors, charge rollers and magnetic rollers, *Proc. IS&T's NIP-10*, pg. 295 (1994)

Biography

Dr. Inan Chen is a consulting scientist on electronic materials, processes and devices, in particular, for applications to electrophotography. He worked at Xerox Research Laboratories in Webster, NY from 1965 to 1998. Recently, he has been engaged in the development of theoretical bases for novel characterization techniques for QEA, Inc. Contact at inanchen@aol.com.

Dr. Ming-Kai Tse founded Quality Engineering Associates (QEA), Inc. in 1987. The company designs and manufactures automated quality control test systems for digital printing technology. He was a professor of Mechanical Engineering at MIT between 1982 and 1989, specializing in manufacturing, non-destructive testing, and quality engineering. Contact at mingkaitse@worldnet.att.net